Ion outflows and artificial ducts in the topside ionosphere at HAARP

G. M. Milikh,[1] E. Mishin,[2] I. Galkin,[3] A. Vartanyan,[1] C. Roth,[4] and B. W. Reinisch[3]

Received 8 July 2010; accepted 6 August 2010; published 23 September 2010.

[1] New results of the DMSP satellite and HAARP digisonde observations during HF heating at the High-Frequency Active Auroral Program (HAARP) facility are described. For the first time, the DMSP satellites detected significant ion outflows associated with 10–30% density enhancements in the topside ionosphere above the heated region near the magnetic zenith. In addition, coincident high-cadence skymaps from the HAARP digisonde reveal field-aligned upward plasma flows inside the *F*-peak region. The SAMI2 2 model calculations are in fair agreement with the observations. **Citation:** Milikh, G. M., E. Mishin, I. Galkin, A. Vartanyan, C. Roth, and B. W. Reinisch (2010), Ion outflows and artificial ducts in the topside ionosphere at HAARP, *Geophys. Res. Lett.*, *37*, L18102, doi:10.1029/2010GL044636.

1. Introduction

[2] Field-aligned density enhancements (ducts) of 1-km-scale or greater guide whistler waves along the geomagnetic field B_0 from lightning sources and VLF transmitters into the magnetosphere and thus play an important role in the radiation belts dynamics [e.g., *Koons*, 1989; *Carpenter et al.*, 2002]. The duct formation mechanism, especially in the topside ionosphere, has not yet been established. Recently, *Milikh et al.* [2008] and *Frolov et al.* [2008] reported on the Demeter and Defense Meteorological Satellite Program (DMSP) satellite observations of artificial ducts in the topside ionosphere during high-power high-frequency (HF) modification experiments at the HAARP and Sura heating facilities, respectively. The modeling results [e.g., *Perrine et al.*, 2006; *Milikh et al.*, 2010] predict that the topside ducts should be accompanied by intense ion outflows, such as detected by the EISCAT UHF incoherent scatter radar during heating experiments at Tromsø [*Rietveld et al.*, 2003]. However, in situ satellite observations of plasma outflows related to artificial ducts have not yet been explored.

[3] This paper describes the first in situ satellite and (remote) digisonde observations of ion outflows associated with artificial ducts during the February 2010 BRIOCHE heating campaign at HAARP. Data was provided by the DMSP satellites F15 and 16 overflying the heated region and by the HAARP digisonde, which used a specially-designed probing schedule to produce skymaps. This was the first application of the skymap to the study of ionospheric HF heating. As a result, for the first time the artificial duct-related ion outflow was determined both in the bottom and topside *F* region.

2. Experiments

[4] The DMSP satellites fly in circular (~840 km altitude) sun-synchronous polar orbits. In this study we use only the SSIES suite of sensors measuring the densities $n_{e,i}$, and drift motions of ionospheric ions and electrons [*Rich and Hairston*, 1994]. The horizontal (V_H) and vertical (V_V) cross-track components of plasma drift are measured within the range of ±3 km/s with one-bit resolution of ΔV = 12 m/s, provided $n_i \geq 5{,}000$ cm^{-3}. It takes 4 seconds to sample the ion composition, while the plasma drift and density are sampled at the rates of 6 and 24 Hz, respectively. The satellite observations were complemented by the HAARP digisonde operated in the skymap mode. Using high-cadence probing schedule and applying several probing frequencies below and above the heating frequency, directional ionograms caused by plasma irregularities were obtained. Those allow us to determine plasma drift velocities in the bottomside *F* region.

[5] During the campaign, there have been four successful overflights by the DMSP F15 and 16 satellites. Table 1 lists their dates and the HF-heating times along with the critical *F*-peak frequency f_0F_2, heating frequency f_0, distance ΔR of the closest approach to the HAARP magnetic zenith (MZ), changes in the field-aligned ion velocity, and the maximum relative deviation of the ion density in the duct $\Delta n_i/n_i$. Here the values ΔR were calculated by using 1 second resolution for DMSP orbits and magnetic zenith coordinates via the magnetic field model. The transmitter was usually turned on 15 min prior to the satellite overflight and operated with the O-mode polarization at the full power of 3.6 MW. The HF beam was pointed at the MZ and had a full width at half-maximum of ≈ 15° and 18° along the magnetic meridian at f_0 = 4.0 and 2.85 MHz with the effective radiative power (ERP) ≈ 650 and 440 MW, respectively. Note that in two cases (4 and 11 February) the heating frequency was close to f_0F_2, whereas on 9 and 10 February f_0 matched the second electron gyro harmonic at an altitude of 230 km.

[6] Figure 1 shows observations made during the 4th and 10th of February. Shown from the top to the bottom are the total ion densities, fractions of O^+ ions, and upward field-aligned ion velocities $V_{up}^{\parallel}$ vs. time relative to T_{mz}. Here T_{mz} is the time of the satellite closest approach to the magnetic zenith of HAARP and $V_{up}^{\parallel} = V_V/\cos(\alpha_0)$, where $\alpha_0 \approx 15°$ is the angle between the vertical and $\mathbf{B}_0$. One can clearly see distinct ion outflows of the width ≤ 100 km (≤ 15 s) about T_{mz}, which is of the order of the HF-heated spot. It should be noted that the spatial profile of the ion outflow is similar to that of the local ion density. Namely the ion density has a bell shape with a peak increase of 30–40%. At

[1]Department of Astronomy, University of Maryland, College Park, Maryland, USA.
[2]Space Vehicles Directorate, Air Force Research Laboratory, Hanscom AFB, Massachusetts, USA.
[3]Center for Atmospheric Research, University of Massachusetts, Lowell, Massachusetts, USA.
[4]AER, Inc., Lexington, Massachusetts, USA.

0094-8276/10/2010GL044636

Table 1. HF-Heating Times and Ionospheric Conditions Which Occur During the Experiments

Vehicle/ Date	Heating Time (UT)	f_oF_2(MHz)	f_o(MHz)	ΔR (km)	Velocity Change (m/s)	$\Delta n_i/n_i$ (%)
F15 02/04	2:10–2:29	4.0	4.0	45	300	30
F16 02/09	17:40–18:00	3.8	2.8	65	100	12
F16 02/10	03:30–03:50	3.6	2.8	10	250	40
F15 02/11	2:00–2:19	4.9	4.25	25	80	8

the same time, the ion outflow leads to ejection of the light H^+ and He^+ ions, thereby increasing the fraction of O^+ ions shown in the middle panel [cf. *Milikh et al.*, 2008]. Observations made during the two other overflights show similar, although weaker, effects (see Table 1).

[7] The cause of the double peak observed on 02/04 has yet to be figured out. It is likely that such a structure is caused by the formation of ring-shaped perturbed region near the F2 peak due to high power pump wave. An example of such dramatic modification can be found in the work of *Pedersen et al.* [2009] where a bright optical rayed ring with a radius of about 70 km was detected. A similar ring could be formed in the topside ionosphere due to the upward plasma drift. Thus a satellite flying with 7.5 km/s velocity could cross such a ring, giving the appearance of two peaks a distance 60 km from the center. The time it would take to cross such a ring is about 10 seconds, which is the same amount of time separating the two peaks on the top and bottom plots in Figure 1.

[8] Figure 2 shows two Doppler sky maps, one made just before the HF-heating the other made two minutes into the heating period. Digisonde uses its echo location capability to detect reflections of transmitted signals from irregular plasma structures in the ionosphere, placing the detected echoes on the skymap plane using their zenith and azimuth angles of arrival [*Reinisch et al.*, 1998]. The color bar shows Doppler shift of each radio beam measured along the line of sight. Negative Doppler shifts indicate the upward motion. Figure 2 (top) shows that prior to heating the irregularities were evenly distributed around the sky view with the Doppler shifts close to zero, which indicates that there is little or no motion of the reflecting irregularities, neither vertical nor horizontal. Two minutes after the heater was turned on, a tight cluster of reflections appeared ± 5° about the MZ (Figure 2, bottom). Note that the yellow color corresponds to negative Doppler shift, i.e., the average upward

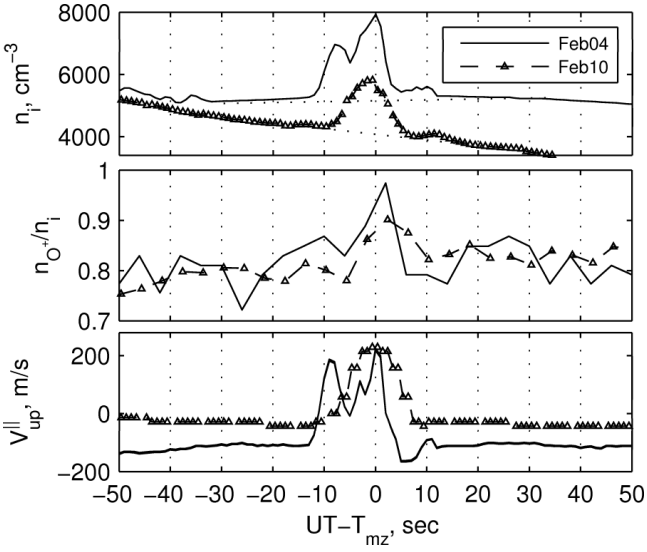

Figure 1. (top) The total ion densities averaged over 1 s, (middle) fractions of O+ ions, and (bottom) 1-s average of upward field-aligned ion velocities vs. time. The time axis is centered on the crossing of the MZ.

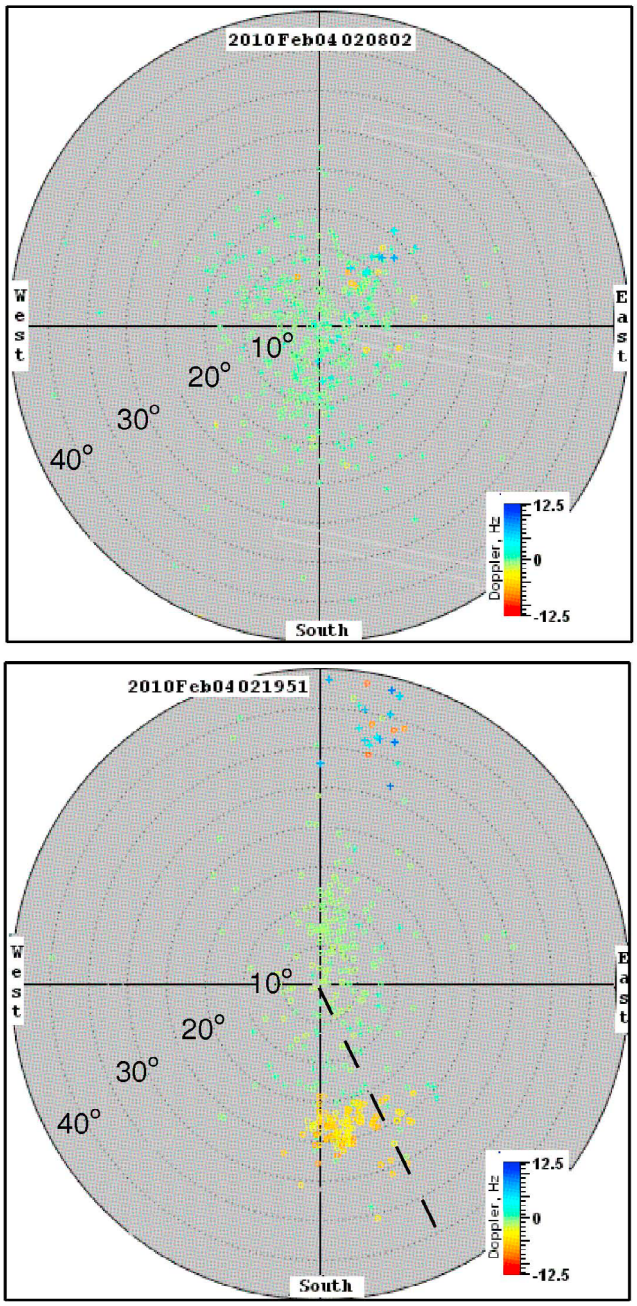

Figure 2. Doppler sky maps from the HAARP digisonde during the heating experiment 02/04/10: (top) 2 min prior and (bottom) 9 min in the HF-heating.

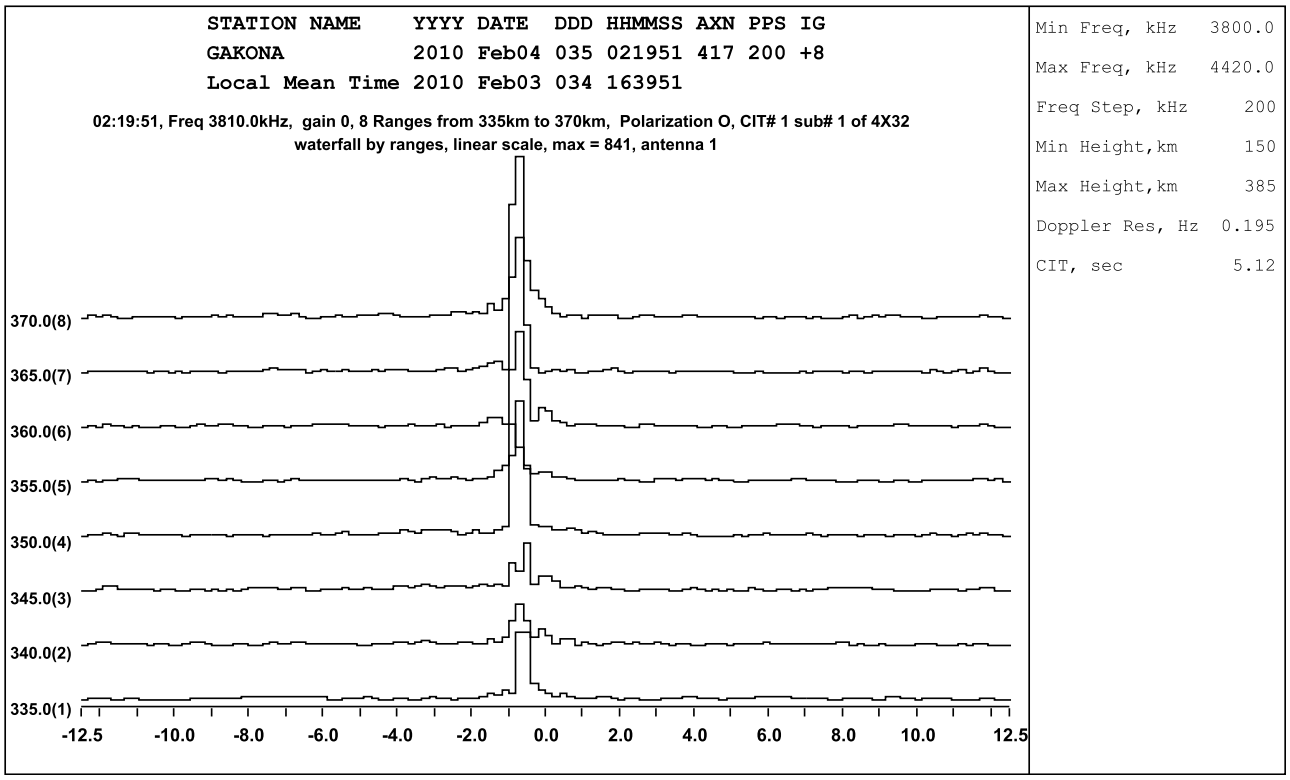

Figure 3. The Doppler shift for a given probing frequency measured at different altitudes between 335 and 370 km.

speed along the magnetic field line. Soon after the heater was turned off the strong "fast" echoes from the MZ disappeared.

[9] Since the detected echoes come from the magnetic zenith, the measured line of sight velocity corresponds to the plasma motion along the magnetic field line. In earlier digisonde studies, *Scali et al.* [1995] had validated the digisonde line of site velocities by comparing collocated incoherent radar measurements with high altitude ionosonde measurements at Sondrestrom, Greenland.

[10] Figure 3 shows Doppler shift Δf_D measured for a given probing frequency f_p at different altitudes. As above, negative Doppler shifts correspond to the upward motion. Figure 3 reveals that the ion velocity increases with altitude. In fact, from Figure 3 one can obtain the upward ion velocity $V_{up}^{\parallel}(h) = c(\Delta f_D / f_p)$ for different altitudes. Thus, we find that $V_{up}^{\parallel}$(335 km) = 55 ± 8 m/s, while $V_{up}^{\parallel}$((370 km) = 70 ± 24 m/s.

3. Discussion and Conclusions

[11] Now we turn to compare the observations against the computational model which is based on the SAMI2 code developed at the Naval Research Laboratory [*Huba et al.*, 2000]. The SAMI2 model is inter-hemispheric and can simulate the plasma along the entire dipole magnetic field line (for the geometry of the model see *Perrine et al.* [2006]). We have modified SAMI2 by introducing in the model a flexible source of electron heating. This source of the electron heating was presented in the form of localized heating rate per electron

$$q = \frac{\mu P}{V n_e} f(x,z) K/s.$$

Here P is the power of the HF heater, V is the volume of the HF absorbed region, n_e is the electron density in this region, while μ is the absorption efficiency. $f(x,z)$ describes the spatial distribution of the HF beam power density [*Milikh et al.*, 2010].

[12] The HF-irradiated spot is taken as a circle centered at x_o having the angular half-widths Θ such that its radius $b = z_{up} \tan \Theta$ and the HF-irradiated volume is $V = \pi a b^2$. It is assumed that electron heating occurs in an altitude range

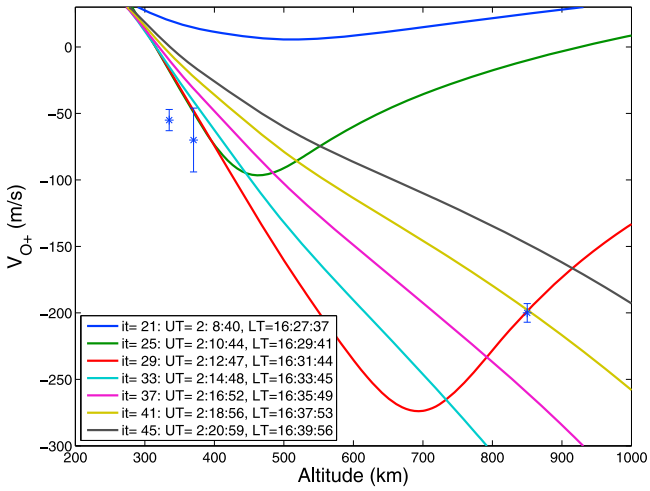

Figure 4. Comparison of the measured outflow velocity with the SAMI2 model results; the time step between the traces is about 2 minutes. The negative velocity corresponds to the upward ion drift. Two bold dots with the bars show the ionosonde observations, while the third dot with the bar shows the DMSP F15 ion velocity.

having the vertical extent a between the wave reflection point and the upper hybrid height, which is dominated by the anomalous absorption (a = 10 km). In this paper we will model the ionospheric conditions at HAARP at the time of our 02/04/10 experiment. We therefore use in the SAMI2 code the corresponding A_p and $F_{10.7}$ indexes, and assume that the heater was turn on at 02:10 UT for 20 minutes. The radiated HF power was 3.6 MW, the facility was operated at a frequency of 4.0 MHz, correspondingly the half power beam width in S–N direction was 14.2°.

[13] The code starts up from empirically determined initial conditions 24 hours before the specific heating time, and runs for 24 hours of 'world clock time'. This practice allows the system to relax to ambient conditions, and reduces noise in the system due to the initialization. Artificial heating continues for some time continuously pumping energy into the electrons at the specified altitude, and the perturbations in ion and electron properties are tracked as they travel along the field line. Then the heater switches off, allowing the ionosphere to relax back to ambient conditions.

[14] Figure 4 shows the ion outflow velocity $V_{up}^{\parallel}$ computed by SAMI2 for the conditions of the 4 February experiment. The set of traces shows the altitude-profile of the ion velocity at different times from the beginning of heating with the time step between the traces about 2 minutes. The HF-heated region was placed near the F_2 peak, and the HF-absorption efficiency was assumed to be 50%, i.e. half of the radio beam energy was released in 10 km thick plasma layer. Such absorption efficiency was used by *Milikh et al.* [2010] in order to reproduce the observations of the vertical ion velocity made by *Rietveld et al.* [2003] at Tromsø. Note that similar volume heating rates were used by *Gustavsson et al.* [2001] and *Mishin et al.* [2004] to explain the artificial emissions induced by the ionospheric HF-heating. Two bold dots with the bars show observations made in the bottomside ionosphere by the ionosonde (see Section 2). The third dot shows the ion velocity from the DMSP F15 satellite in the topside ionosphere. Note that the best agreement occurs between the satellite observations and the model profile, corresponding to 18 minutes of heating, which is close to the fly over time of DMSP. However, note that the modeling results are slightly lower than the observed values.

[15] To summarize, the ion outflows related to artificial ducts created by HF-heating at HAARP were measured simultaneously in the topside ionosphere by the DMSP satellites and in the bottomside ionosphere by the HAARP ionosonde. The SAMI2 simulation results are in fair agreement with the observations.

[16] **Acknowledgments.** We thank Dennis Papadopoulos for helpful discussions. HAARP is a Department of Defense project operated jointly by the U.S. Air Force and U.S. Navy. G.M. and A.V. were supported by DARPA via a subcontract N684228 with BAE Systems and also by the ONR grants NAVY.N0017302C60 and MURI N000140710789. E.M. was supported by the Air Force Office of Scientific Research. I.G. and B.W.R. were supported by USAF grant FA8718-L-0072 of the AF Research Laboratory. We are also very thankful for Lee Snyder's help with the digisonde measurements.

References

Carpenter, D., et al. (2002), Small-scale field-aligned plasmaspheric density structures inferred from the Radio Plasma Imager on IMAGE, *J. Geophys. Res.*, *107*(A9), 1258, doi:10.1029/2001JA009199.

Frolov, V., V. Rapoport, G. Komrakov, A. Belov, G. Markov, M. Parrot, J. Rauch, and E. Mishin (2008), Density ducts formed by heating the Earth's ionosphere with high-power HF radio waves, *JETP Lett.*, *88*, 790–794, doi:10.1134/S002136400824003X.

Gustavsson, B., et al. (2001), First tomographic estimate of volume distribution of HF-pump enhanced airglow emission, *J. Geophys. Res.*, *106*, 29,105–29,123, doi:10.1029/2000JA900167.

Huba, J., G. Joyce, and J. Fedder (2000), Sami2 is another model of the ionosphere (SAMI2): A new low-latitude ionosphere model, *J. Geophys. Res.*, *105*, 23,035–23,053, doi:10.1029/2000JA000035.

Koons, H. (1989), Observations of large-amplitude, whistler-mode wave ducts in the outer plasmasphere, *J. Geophys. Res.*, *94*, 15,393–5,397, doi:10.1029/JA094iA11p15393.

Milikh, G., K. Papadopoulos, H. Shroff, C. Chang, T. Wallace, E. Mishin, M. Parrot, and J. Berthelier (2008), Formation of artificial ionospheric ducts, *Geophys. Res. Lett.*, *35*, L17104, doi:10.1029/2008GL034630.

Milikh, G., A. Demekhov, K. Papadopoulos, A. Vartanyan, J. Huba, and G. Joyce (2010), Model for artificial ionospheric duct formation due to HF heating, *Geophys. Res. Lett.*, *37*, L07803, doi:10.1029/2010GL042684.

Mishin, E. V., W. J. Burke, and T. Pedersen (2004), On the onset of HF-induced airglow at magnetic zenith, *J. Geophys. Res.*, *109*, A02305, doi:10.1029/2003JA010205.

Pedersen, T., et al. (2009), Optical ring formation and ionization production in high-power HF heating at HARP, *Geophys. Res. Lett.*, *36*, L18107, doi:10.1029/2009GL040047.

Perrine, R., G. Milikh, K. Papadopoulos, J. Huba, G. Joyce, N. Swisdak, and Y. Dimant (2006), An interhemispheric model of artificial ionospheric ducts, *Radio Sci.*, *41*, RS4002, doi:10.1029/2005RS003371.

Reinisch, B., J. Scali, and D. Haines (1998), Ionospheric drift measurements with ionosondes, *Ann. Geofis.*, *41*, 695–702.

Rich, F., and M. Hairston (1994), Large-scale convection patterns observed by DMSP, *J. Geophys. Res.*, *99*, 3827–3844, doi:10.1029/93JA03296.

Rietveld, M., M. Kosch, N. Blagoveshchenskaya, V. Kornienko, T. Leyser, and T. Yeoman (2003), Ionospheric electron heating, optical emissions, and striations induced by powerful HF radio waves at high latitudes: Aspect angle dependence, *J. Geophys. Res.*, *108*(A4), 1141, doi:10.1029/2002JA009543.

Scali, J. L., B. W. Reinish, C. J. Heinselman, and T. Bullet (1995), Coordinated digisonde and incoherent scatter radar F region drift measurement at Sondre Stromfjord, *Radio Sci.*, *30*, 1481–1498, doi:10.1029/95RS01730.

I. Galkin and B. W. Reinisch, Center for Atmospheric Research, University of Massachusetts, Lowell, MA 01854, USA.

G. M. Milikh and A. Vartanyan, Department of Astronomy, University of Maryland, College Park, MD 20742, USA.

E. Mishin, Space Vehicles Directorate, Air Force Research Laboratory, Hanscom AFB, MA 01731, USA.

C. Roth, AER, Inc., 131 Hartwell Ave., Lexington, MA 02421, USA.